Article

Selective Label-Free Electrochemical Aptasensor Based on Carbon Nanotubes for Carbendazim Detection

Constanza J. Venegas *[ID], **Luna Rodríguez** and **Paulina Sierra-Rosales** *[ID]

Programa Institucional de Fomento a la Investigación, Desarrollo e Innovación, Universidad Tecnológica Metropolitana, Ignacio Valdivieso 2409, P.O. Box 8940577, San Joaquín, Santiago 8320000, Chile
* Correspondence: cvenegasa@utem.cl (C.J.V.); psierra@utem.cl (P.S.-R.)

Abstract: One of the most widely used pesticides in Chile is carbendazim (CBZ), which in agriculture is used to protect crops from fungal diseases that commonly occur in rice, vegetable, and fruit crops. However, prolonged exposure to it, and its high persistence, can cause adverse health effects. Therefore, it is necessary to determine the presence of CBZ through rapid detection methods in food samples to prevent ingestion and exposure to this pesticide at risk concentrations. In this work, a label-free electrochemical aptasensor based on functionalized carbon nanotubes was prepared for CBZ detection. The carbodiimide reaction between the amino-terminated aptamer and the carboxylic groups of carbon nanotubes achieved the covalent immobilization of the aptamer. The immobilized aptamer changed its conformation when it detected CBZ and blocked access to the redox mediator on the electrode surface, resulting in a measurable decrease in the voltammetric response. Under the optimal conditions, the aptasensor featured a linear detection range between 1.0 and 50.0 nM, with a detection limit of 4.35 nM. Moreover, the aptasensor exhibited good selectivity for CBZ, among other pesticides, and good repeatability. For CBZ detection in tomatoes, the aptasensor accurately measured CBZ content in a sample prepared using the standard addition method. This work provides a simple, rapid, sensitive, and selective biosensor for CBZ detection and quantification in food samples.

Keywords: electrochemical aptasensor; carbendazim; carbon nanotubes

1. Introduction

Carbendazim (CBZ) is a systemic fungicide widely used in agriculture to eliminate fungal diseases. It has a long half-life due to its benzimidazole ring. Its persistence can cause environmental damage in both water and soil, and its decomposition can take between 3 to 6 months on grass, 6 to 12 months on bare soil, and up to 25 months in water under aerobic and anaerobic conditions [1,2]. In plants, CBZ is absorbed by the roots, seeds, and leaves. These plants can then be consumed by animals and humans and cause short and long-term harmful health effects. With this, recent studies have reported CBZ's negative impact on human fertility [3] and found evidence of its embryotoxicity [4]. Similar adverse health impacts have been observed in fish and other aquatic organisms [5]. As a result, this fungicide is considered highly toxic, carcinogenic, and teratogenic [6]. Therefore, it is necessary to determine the presence of CBZ through rapid detection methods in food samples to prevent ingestion and exposure to this pesticide at risk concentrations.

Several methods have been developed for the detection of CBZ based on mass spectroscopy [7], UV–visible spectrometry [8], Raman scattering [9], fluorescence spectroscopy [10], capillary electrophoresis [11], and high-performance liquid chromatography (HPLC). HPLC is the main analytical technique for detecting and quantifying pesticides due to its high sensitivity and reliability. For example, an HPLC-based method combining dispersive liquid–liquid micro-extraction and fluorescence spectroscopy enabled the detection of CBZ for concentrations as low as 0.5 ng/mL [12]. While these techniques have high sensitivity, good detection limits, and high reliability, they present several disadvantages.

These disadvantages include requiring sophisticated, bulky instrumentation, specialized technicians, high cost, long measurement times, multistep sample pretreatment steps, complex analysis, and large volumes of solvents, precluding these techniques from being widely deployed in the field [13]. Thus, it is necessary to develop new sensitive, fast, and low-cost methods to detect CBZ in food samples.

In this sense, biosensors represent an innovative and promising technology due to their low cost, rapid response times, high sensitivity and selectivity, ease of handling, and multifunctionality [1]. Biosensors are analytical devices that contain two main components: a biological recognition element (enzymes, oligonucleotides, antibodies, aptamers, or cells) and a transducer (an electrode, in this case). Due to their lower cost of production, higher stability, and higher or equal selectivity and affinity towards the target analyte, aptamers have been extensively used in basic research, clinical diagnostics, environmental protection, and food safety [14–16]. Aptamers are artificial single-stranded DNA or RNA short sequences that can specifically bind to target molecules by folding into distinct structures. These targets range from small molecules and metals to proteins, viruses, and cells [15]. This capability has enabled aptamers to detect food contaminants, environmental pollutants, disease markers, pathogenic microorganisms, and drug molecules [16]. Furthermore, aptamers can be easily synthesized and labeled without affecting the affinity towards their ligands, are more stable when compared to antibodies, provide large dynamic concentrations, and can be used in a wider range of experimental conditions [17,18]. Additionally, aptamers are easily modified with functional groups, which is useful for labeling and surface immobilization.

For CBZ, the development of electrochemical aptasensors is in the early stages [19–22]. In 2016, Eissa et al. [19] successfully identified two aptamers highly specific for CBZ and developed an impedimetric aptasensor via self-assembly of thiol-modified aptamer on gold electrodes. The aptasensor showed good analytical performance with a low LOD (8.2 pg/mL) and could detect CBZ in food matrices. In 2019, Zhu et al. [20] reported a carbon nanohorns/gold nanoparticle composite impedimetric aptasensor for the detection of CBZ. The thiolated aptamer was immobilized by the Au-S bond on the AuNPs and achieved a LOD of 0.5 pg/mL; the sensor also detected CBZ in food samples. Two years later, Wang et al. [21] developed an aptasensor based on a colloidal mixture of boron nitride nanocrystals and gold nanoparticles. The nanomaterials were deposited on a glassy carbon electrode (GCE), and a single-stranded oligonucleotide label with methylene blue was incorporated on the electrode to achieve the hybridization of the aptamer. The final aptasensor was capable of detecting CBZ with a LOD of 0.019 ng/mL and was tested in food and water samples. Recently, Khosropour et al. [22] developed an aptasensor based on gold nanoparticles/graphene nanoribbons/MOF/GCE to detect CBZ in water samples. The aptasensor showed a LOD value of 0.4 fM, the lowest LOD value reported in the literature. Despite the excellent analytical parameters that all four aptasensors demonstrated, none allow their use in the field. In this context, an aptasensor based on screen-printed electrodes will enable a portable sensor for field applications.

Here, we report for the first time a simple and portable electrochemical aptasensor based on carbon nanotubes for detecting CBZ with LOD values similar to those obtained by HPLC. The amino-terminated aptamer was immobilized on screen-printed electrodes modified with carbon nanotubes via carbodiimide reaction. The selectivity, reproducibility, and stability of the aptasensor were tested. Finally, the applicability of the aptasensor was demonstrated by detecting CBZ in a tomato sample.

2. Materials and Methods

2.1. Reagents and Materials

Monobasic potassium phosphate (KH_2PO_4, 99%), dibasic potassium phosphate (K_2HPO_4, 98%), tris(hydroxymethyl)aminomethane (Tris, 99.8%), N-(3-dimethyl aminopropyl)-N′ethylcarbodiimide hydrochloride (EDC, 98%), N-hydroxysuccinimide (NHS, 98%), bovine serum albumin (BSA, 98%), Carbendazim (CBZ, 97%), and Nafion® (5 wt%) were purchased

from Sigma Aldrich. Potassium chloride (KCl), potassium ferrocyanide ($K_4Fe(CN)_6 \times H_2O$, 98.5–102.0%), potassium ferricyanide ($K_3Fe(CN)_6$, 99%) ethylenediaminetetraacetic acid (EDTA), hydrochloric acid (HCl, 37%), sodium hydroxide (NaOH, $\geq$98%), and nitric acid (HNO_3, 65%) were obtained from Merck. Methanol (Winkler), multiwalled carbon nanotubes (CNT, 1–5 μm long and 30 $\pm$ 15 nm diameter) (NanoLab, Waltham, MA, USA), and ethanol (Soviquim) were used for experiments. Double deionized water (18.6 MΩ) was used. The amine terminal aptamer was synthesized by Fermelo Biotec (Santiago, Chile) and its sequence was [19]:

5′-/NH_2/C_6-CGA CAC AGC GGA GGC CAC CCG CCC ACC AGC CCC TGC AGC TCC TGT ACC TGT GTG TGT G-3′.

The aptamer (100 μM) was prepared with Tris (10 mM)–EDTA (0.1 mM) (TE) buffer solution at pH 8.0 and re-suspended at 55 °C for 5 min. It was stored at −20 °C. The CBZ was dissolved with methanol and diluted with phosphate buffer solution (PBS, pH 7.4) to obtain a stock solution with different concentrations.

2.2. Apparatus

Scanning electron microscope images were obtained using a Gemini 360 ZEISS field emission microscopy (FE-SEM) to characterize the electrodes before and after modification with CNTs dispersion.

All electrochemical measurements (cyclic voltammetry (CV) and differential pulse voltammetry (DPV)) were performed on a CHI650E potentiostat (CH Instruments). The parameters of CV in $[Fe(CN)_6]^{3-/4-}$ were as follows: scan potential 0.7 to −0.1 V, 50 mV/s, and the equilibrium time was 2 s. DPV parameters in $[Fe(CN)_6]^{3-/4-}$ were: scan potential 0.7 to −0.1 V, 0.05 V amplitude, 0.06 sec pulse width. Screen-printed carbon electrodes (SPCE) (DRP-110, DropSens) and commercial AuNP-modified SPCE (SPAuNPE) (DRP-110GNP, DropSens) were used. A specific cable connector (DRP-CAC, DropSens) was used between the electrodes and the potentiostat. All measurements were performed in triplicate.

2.3. Fabrication of the Aptasensor

Commercial CNTs were oxidized according to the procedure of Cañete et al. [23]. Briefly, 250 mg of CNTs were immersed in 100 mL of 7.0 M HNO_3, and refluxed for 6 h. The oxidized CNTs (CNT-COOH) were filtered and washed with distilled water and dried under vacuum. CNT-COOH were dispersed at 1.0 mg/mL with Nafion® 0.2% in ethanol by sonication for 5 min. Then, the screen-printed carbon electrode was modified with 15 μL of CNT dispersion on the surface of the working electrode and allowed to dry at room temperature. Next, carboxylic groups of CNTs were activated via a carbodiimide reaction adding a certain volume of EDC (2.0 mM) and NHS (5.0 mM) in 0.1 M PBS (pH 7.4) for 1 h. After -COOH activation, the electrode was rinsed and the aptamer (AP-NH_2, 10.0 μM) was incubated for 12 h at 4 °C to achieve the covalent immobilization, then washed with TE buffer. Finally, at room temperature, 1.0% BSA was added for 1 h and washed with 0.1 M PBS, pH 7.4. The steps involved in fabricating the electrochemical aptasensor are depicted in Scheme 1.
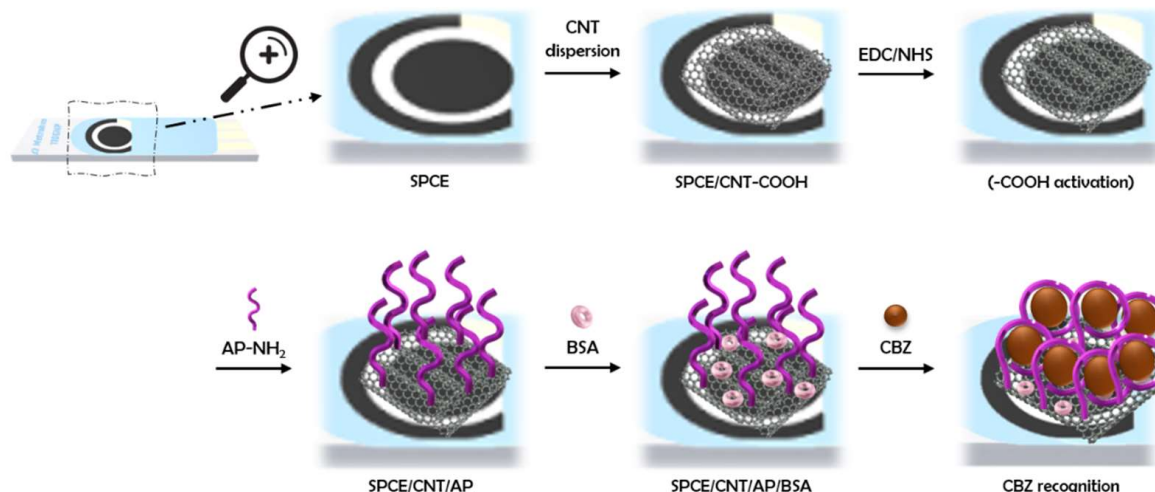
2.4. CBZ Detection

To detect CBZ, 15 μL of CBZ was cast on the aptasensor in a fixed concentration. After incubation for 30 min at room temperature, the aptasensor was washed with 0.1 M PBS (pH 7.4), and the voltammetric response was measured. The calibration curve was obtained by plotting the faradic current vs. CBZ concentration. All experiments were performed at room temperature and in triplicate.

2.5. Real Sample Preparation

Tomatoes were purchased from a local supermarket (Santiago, Chile). Tomatoes were washed and chopped into small pieces using a blender. Subsequently, the sample was

centrifuged at 10,000 rpm for 10 min. Then, the extract was filtered at 0.45 μm and enriched with CBZ in 0.1 M PBS (pH 7.4). The aptasensor was put into an electrolytic cell, and DPV was used for quantitative analysis. The parameters used were the same as those described in Section 2.2.

Scheme 1. Schematic illustration of the fabrication of an electrochemical aptasensor for CBZ detection.

3. Results and Discussion

3.1. Aptasensor Fabrication

The fabrication of the aptasensor included three critical stages to maintain the aptamer functionality for CBZ detection (Scheme 1):

- Surface modification of the electrode with CNT-COOH
- Covalent immobilization of the aptamer-NH$_2$ to CNT-COOH (via EDC/NHS reaction)
- Incorporation of bovine serum albumin (BSA) to block unspecific adsorption

Several variables were optimized for the analytical performance of the aptasensor: (a) concentration of the CNT dispersion; (b) concentration of the dispersant agent (Nafion); (c) activation time of CNT-COOH by EDC/NHS reaction; (d) concentration of the aptamer-NH$_2$; (e) incubation time of the aptamer-NH$_2$; (f) presence of blocking agent (BSA) and (g) electrode substrate. Table 1 summarizes the ranges and the parameters selected for the fabrication of the aptasensor. All the variables were optimized by cyclic voltammetry in 5.0 mM [Fe(CN)$_6$]$^{3-/4-}$ in 0.1 M PBS pH 7.4.

Table 1. Optimization of the variables in the fabrication of the aptasensor.

Variable	Range Tested	Selected Value
The concentration of CNT dispersion, mg/mL	0.5–1.0–2.0	1.0
Concentration of Nafion® in the dispersion, % (v/v)	0.05–0.1–0.2	0.2
Activation time of CNT-COOH by EDC/NHS reaction, hours	1–2	1
The concentration of the Aptamer-NH$_2$, μM	1.0–5.0–10.0–20.0	10.0
The incubation time of the Aptamer-NH$_2$, hours	1–5–12–24–48	12
Blocking agent (BSA)	Presence and absence	Presence
Electrode surface	SPAuNPE and SPCE	SPCE

A uniform CNT-COOH dispersion coating enhances the electrical conductivity of the electrode surface and is particularly important for the aptasensor performance because the immobilization of the aptamer, a non-conductive biomolecule, will decrease the electrical response of the electrode. Therefore, the concentration of the CNT-COOH dispersion was

optimized for high current values before aptamer immobilization (Figures 1a and S1, and Table S1).
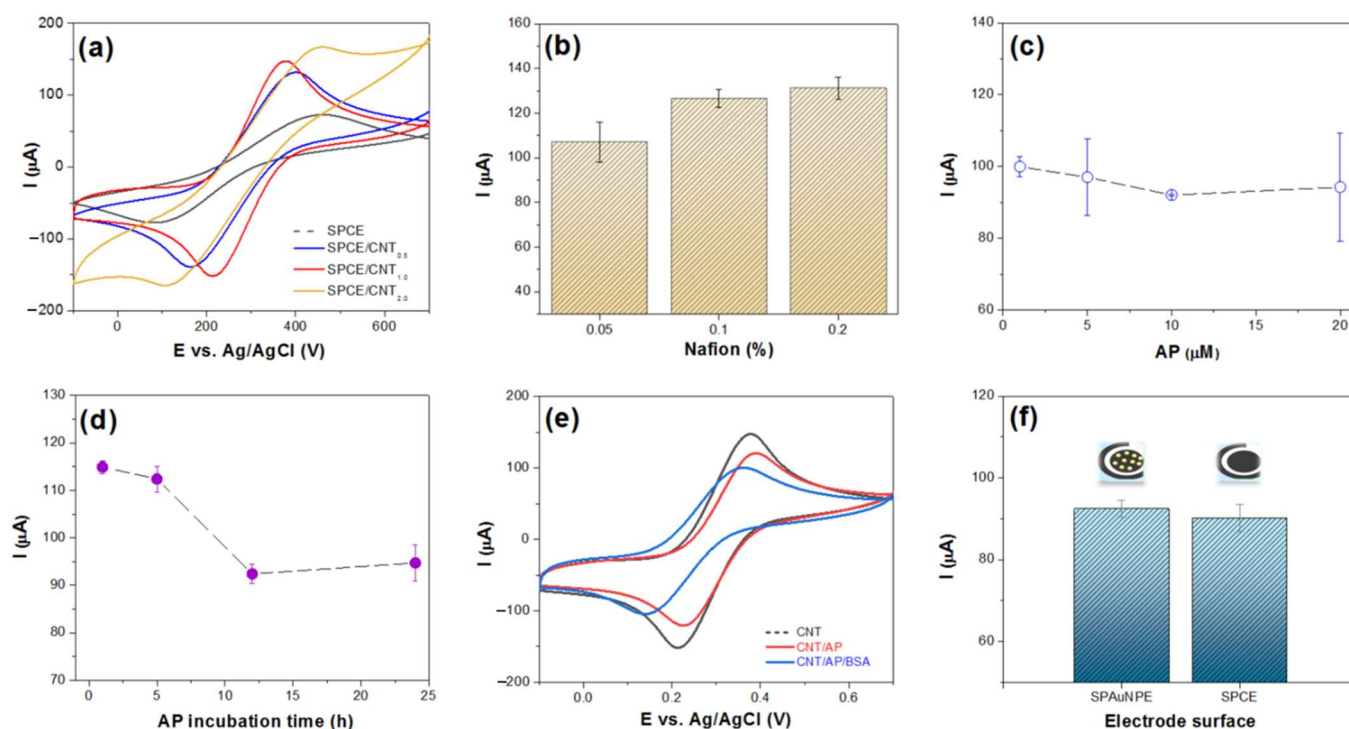

Figure 1. Optimization of the variables in the fabrication of the aptasensor in 5.0 mM $(Fe(CN)_6)^{4-/3-}$ in 0.1 M PBS + 0.1 M KCl (pH 7.4): (**a**) cyclic voltammograms of bare SPCE and modified SCPE with different concentration of CNT; (**b**) concentration of Nafion in 1.0 mg/mL dispersion with CNT; (**c**) aptamer concentration; (**d**) incubation time of 10.0 µM of aptamer; (**e**) presence/absence of BSA, and (**f**) different electrodes surfaces used as support. All measurements were performed in triplicate.

Figure 1a shows the cyclic voltammograms obtained with bare SPCE and SPCEs modified with different concentrations of CNTs. For the bare SPCE, a pair of redox peaks for $[Fe(CN)_6]^{3-/4-}$ was observed with a peak potential difference (ΔE_P) of 365 mV, indicating that SPCE is not a good substrate for the reaction of the redox probe. This can be related to the carbon ink used to prepare the electrodes. This ΔE_P agrees with other articles that used SPCEs as working electrode [24–26]. Compared to the bare SPCE, the cyclic voltammogram of the electrode modified with a dispersion of 0.5 mg/mL of CNTs $(SPCE/CNT_{0.5})$ showed an increase in current intensity and a decrease in ΔE_P (from 365 mV to 237 mV). This indicates that CNTs facilitated the electron transfer rate of the redox mediator even at low concentrations. With 1.0 mg/mL of CNTs $(SPCE/CNT_{1.0})$, the redox profile of $[Fe(CN)_6]^{3-/4-}$ becomes more reversible, with a ΔE_P of 156 mV and presents higher current values. Finally, the increment of CNTs on the electrode surface to 2.0 mg/mL $(SPCE/CNT_{2.0})$ showed a voltammetric profile that was more resistive and less reversible, which is verified with the ΔE_P value (352 mV). As shown in Figure S1a, both 1.0 mg/mL and 2.0 mg/mL showed high current values compared to 0.5 mg/mL, but 1.0 mg/mL had the lowest error. The current values increased with the concentration of CNTs, but at 2.0 mg/mL, the current increased marginally. Additionally, cyclic voltammograms were obtained for each dispersion before and after the immobilization of the aptamer. It is expected that the immobilization of the aptamer causes a decrease in the current, mainly explained by an electrostatic repulsion interaction between the aptamer and the redox mediator [26]. This effect was observed only when CNTs dispersion was 0.5 and 1.0 mg/mL (Figure S1b–d). With these results, 1.0 mg/mL was chosen for the next experiments.

The concentration of Nafion in the dispersion of CNTs was also evaluated (Figure 1b). The cyclic voltammetric profiles revealed reversible behavior for higher concentrations of Nafion (Figure S2). The CNT dispersion prepared with 0.1% and 0.2% Nafion showed high current values and low error. However, a dispersion with 0.2% Nafion resulted in better dispersion and higher uniformity on the electrode surface (not shown), resulting in a lower ΔEp and higher Ip (Table S2). Therefore, 0.2% of Nafion was selected for the dispersion.

The reaction with EDC/NHS achieved the covalent immobilization of the aptamer. In a previous work [27], we successfully functionalized MWCNTs with DNA through the covalent attachment of an oligonucleotide. The carboxylic acid groups of the CNTs were activated with carbodiimide, and the reaction was conducted in aqueous media and stirring. In this case, we used the same protocol to activate the -COOH groups, but the covalent functionalization was achieved on the modified electrode without stirring. The EDC/NHS was deposited on the electrode for 1 and 2 h, and then the aptamer was immobilized. As seen in Table S3, with 1 h of activation with EDC/NHS, the aptasensor reached a lower ΔEp and an RSD of 3.2%. Thus, 1 h was chosen as the optimum time.

As the primary biological recognition element, the aptamer loading used in the sensor fabrication was optimized. Figure 1c shows the effect of the aptamer concentration on the aptasensor response. Similar current values are observed for all concentrations used (Table S4). Since the covalent immobilization depends on the availability of -COOH groups in the functionalized CNTs, these results could indicate that the surface of the CNTs was functionalized sparingly with -COOH groups and, therefore, the maximum amount of aptamer immobilized was rapidly reached. Our results indicate that 10 μM of the aptamer is enough to obtain reproducible results (RSD 2.8%).

The incubation time of 10 μM of aptamer was evaluated for a range from 1 to 24 h (Figure 1d, Table S5). In this case, the immobilization is expected to decrease the current intensity by reducing the effective electrode surface area and impeding the electronic transfer process of the redox mediator. Figure 1d shows the lowest current and low RSD (2.3%) within 12 h. Therefore, 12 h was selected as the optimal incubation time.

To avoid non-specific bonding on the surface, molecules such as bovine serum albumin (BSA) or casein are used as blocking agents [28–31]. Figure 1e shows the voltammetric profile of the electrode modified with CNT, SPCE/CNT-AP, and SPCE/CNT-AP/BSA. As expected, after the aptamer immobilization, a decrease in current is observed compared to SPCE/CNT. A further decrease in current intensity was observed when BSA was added, associated with blocking non-specific interactions. Additionally, the processes become less reversible. These results indicate that BSA is effective as a blocking agent.

Finally, using the optimized conditions, two different electrodes were tested as the substrate for the aptasensor (Figure 1f, Table S6). To determine if the presence of AuNPs improved the response of the sensor, screen-printed carbon electrodes with gold nanoparticles (SPAuNPE) and screen-printed carbon electrodes (SPCE) were compared. The results show that the SPCE presents current values similar to those obtained with SPAuNPE, despite having a combination of nanomaterials that could synergize their electrocatalytic properties. For a better understanding, SEM images of the bare and modified electrodes were conducted. Figure 2 shows SEM micrographs for the surfaces of each electrode before and after modification with CNTs. For SPAuNPE electrodes (Figure 2c), CNTs seem to be mixed with the AuNPs forming a uniform film on the electrode surface. In the SPCE electrode (Figure 2d), the CNTs are uniformly dispersed over the electrode surface, similar to what was observed for SPAuNPE. The current observed for both electrodes was similar, as well as the RSD (Table S6). SPCE is cheaper than SPAuNPE, and adding AuNPs did not significantly improve performance, so SPCE was chosen as the electrode for the aptasensor.

3.2. Carbendazim Recognition Assessment

After optimizing the aptasensor, the CBZ binding time was studied by differential pulse voltammetry (DPV). The binding of the analyte to the probe is expected to generate a conformational change in the aptamer, decreasing the electrochemical response as the

concentration increases [32]. Binding times of 5, 30, 60, and 120 min were evaluated (Figure 3a, Table S7). In Figure 3a, the current intensity rapidly decreases with time, as expected, demonstrating a successful recognition of CBZ by the aptamer probe. After 30 min of interaction, the current reaches a constant value, which slightly increases at 120 min. To ensure the interaction without having a very long reaction time, 30 min was chosen as the optimal AP-CBZ binding time.
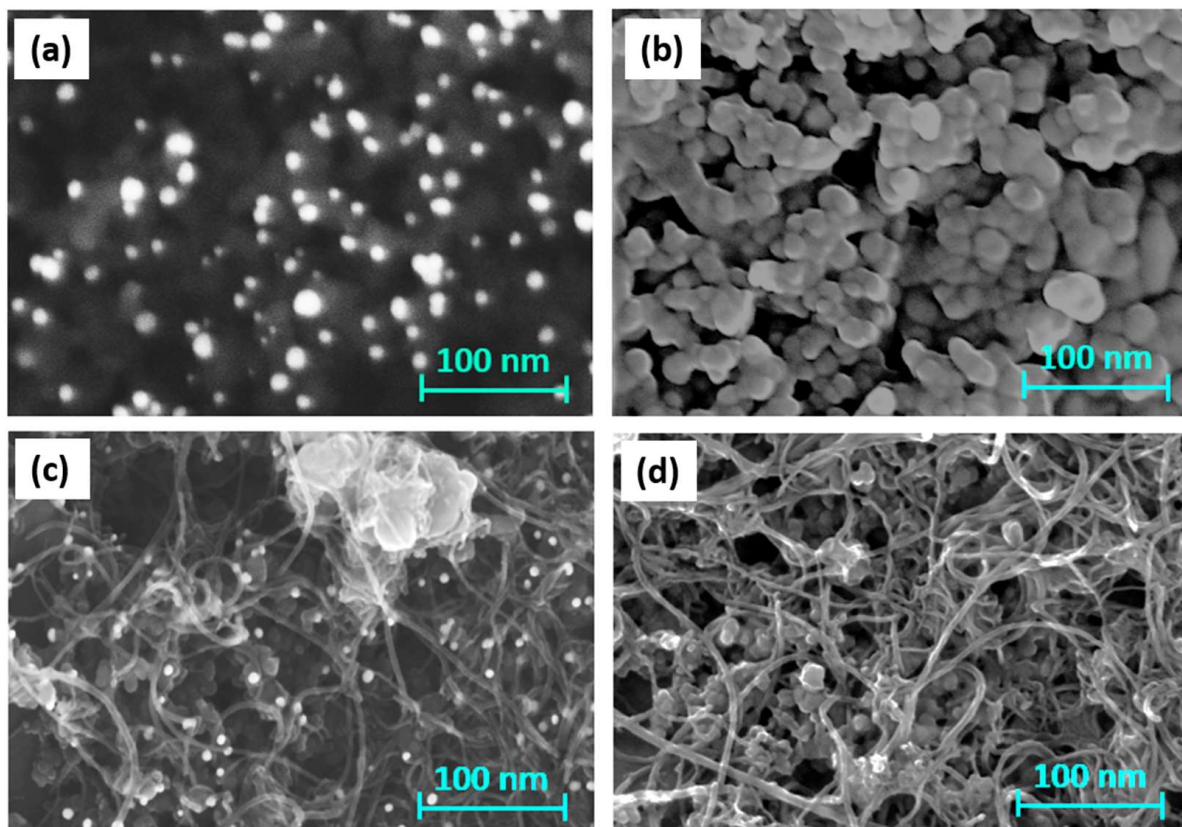

Figure 2. SEM images of screen-printed electrodes before and after modification with CNTs: (**a**) bare SPAuNPE; (**b**) bare SPCE; (**c**) SPAuNPE/CNT; and (**d**) SPCE/CNT.
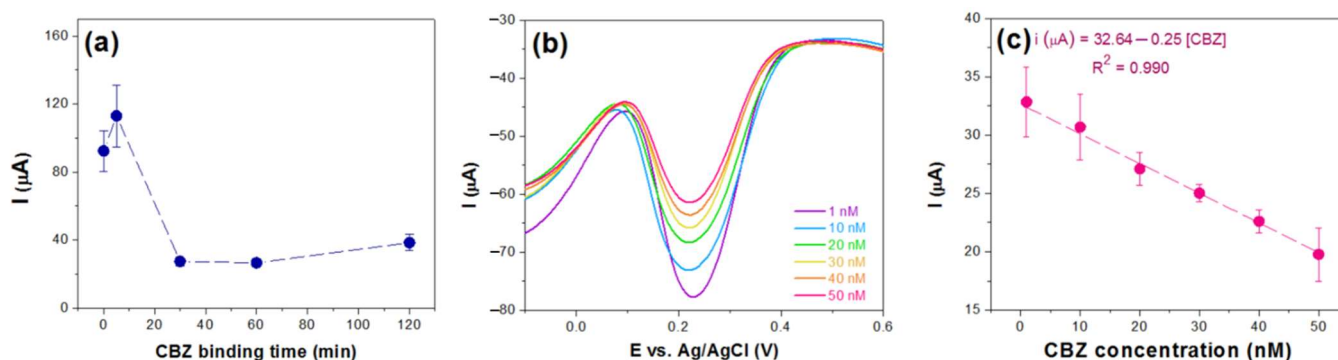

Figure 3. (**a**) Influence of the CBZ incubation time on the aptasensor; (**b**) DP voltammograms of 1.0 mM CBZ in 0.1 M PBS (pH 7.4) with different concentrations of CBZ; (**c**) calibration plot of (**b**). All measurements were performed in triplicate.

To verify that CBZ recognition occurs with the aptamer covalently immobilized to the surface by the reaction with EDC/NHS, the CBZ recognition response was compared with aptasensors constructed in the absence of EDC/NHS (Figure S3). When EDC/NHS is not incorporated, the -COOH groups of the carbon nanotubes are not activated, and the

aptamer is directly adsorbed on the electrode. In this case, when the aptamer recognizes the CBZ, its interaction is favored, which would cause desorption of the CBZ-AP system. The desorption generates free spaces on the electrode surface, favoring the redox process of the mediator with the surface, which increases the current. In Figure S3a,b, it is observed that in the absence of EDC/NHS, the current is higher than in the presence of EDC/NHS (17% increase), corroborating the covalent immobilization of the aptamer by the EDC/NHS reaction.

Under the optimal conditions, the response of the aptasensor with varying CBZ concentrations was evaluated by DPV (Figure 3b). The voltammograms' current intensities decreased as the carbendazim concentration increased. The calibration plot (Figure 3c) shows a linear range between 1.0 and 50.0 nM, with a regression equation of I(μA) = 32.64–0.25 (CBZ) (R^2 = 0.990). The limit of detection (LOD) was calculated as 4.35 nM (0.83 ng/mL) ($LOD = \frac{3\sigma}{S}$).

The analytical performance of the sensor was compared with other aptasensors developed for CBZ. As shown in Table 2, the aptasensor developed here is the only one based on carbon nanotubes instead of gold surfaces (solid electrodes or nanoparticles) and used SPCE as the transducer. SPCE and functionalized carbon nanomaterials enabled a simple strategy to immobilize the aptamer on CNTs covalently and present an alternative immobilization strategy to those published, primarily based on hybridization with label-oligonucleotide and self-assembly monolayer formation. Although our aptasensor sensor features a higher LOD than the aptasensors immobilized on gold, the calculated LOD is within the same range as HPLC with fluorescence detector, but with the added advantages of being portable and featuring analysis times on the order of minutes.

3.3. Selectivity, Reproducibility, and Stability of the Aptasensor

The selectivity of the aptasensor was evaluated by comparing the detection responses of CBZ of other pesticides, including trifluralin (TRI), atrazine (ATR), glyphosate (GPS), and their mixtures. The concentration of each interfering agent (300 nM) was 10 times higher than that of CBZ (30 nM). As shown in Figure 4a, in the presence of CBZ, the electrochemical response of the aptasensor decreased due to the conformational change of the aptamer. However, when other pesticides such as TRI, ATR, and GPS were present, the electrochemical response did not decrease. Only the mixture of pesticides with CBZ showed a decrease in current, demonstrating the high selectivity of the aptasensor.

The reproducibility of the aptasensor was assessed with three different aptasensors (Figure 4b), and the relative standard deviation (RSD) was found to be 2.5%.

To estimate the stability, a batch of developed aptasensors was stored at 4 °C, and the stability test was performed over several days. As shown in Figure 4c, the initial current varies slightly as the storage time goes by. The current on the eighth day corresponds to 95.3% of the current on the first day, indicating high stability.
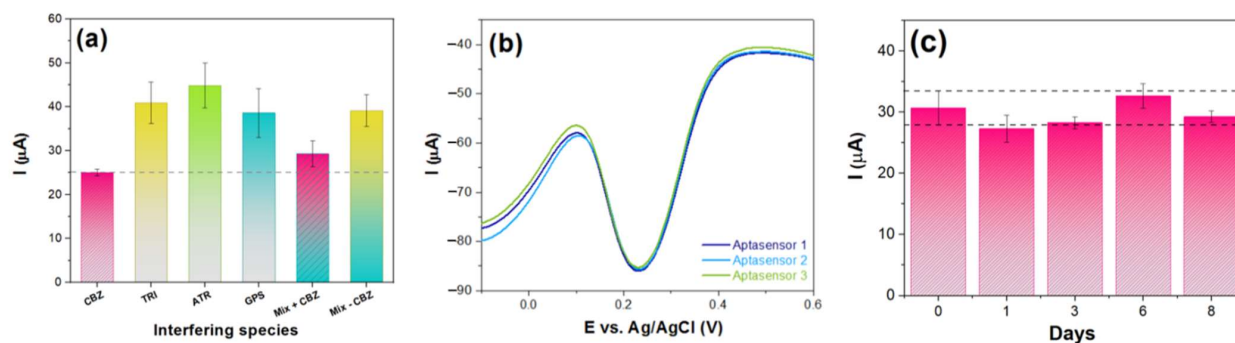

Figure 4. (**a**) Evaluation of the selectivity of the aptasensor against different interfering pesticides; (**b**) evaluation of the reproducibility of the aptasensors with 30 nM CBZ in 0.1 M PBS (pH 7.4), and (**c**) evaluation of the stability of the aptasensor for CBZ after stored for 1–8 days. All measurements were performed in triplicate.

Table 2. Comparison of the performance of the proposed aptasensor with reported electrochemical aptasensor.

Electrode	Aptamer Immobilization Strategy	Aptasensor Fabrication Time	Technique	Linear Range (ng/mL)	LOD (ng/mL)	Ref.
GCE/BN/AuNPs/CP/MCH/AP-SH	Hybridization with label-oligonucleotide	MB-CP probe (1 h) + MCH (1 h) + Aptamer (overnight)	DPV	0.10–$1 \cdot 10^5$	0.019	[21]
Au/AP-SH/MCH	Self-assembly monolayer formation	Aptamer (24 h) + MCH (30 min)	EIS	0.01–10	0.0082	[19]
GCE/CNHs/AuNPs/AP-SH/MCH	Self-assembly monolayer formation	Aptamer (10 h) + MCH (1 h)	EIS	0.001–1	0.0005	[20]
GCE-MOF/GNR@AuNP/cAP-SH/AP/MCH	Hybridization	cAP-SH (30 min) + Hybridization (60 min) + MCH (1 h)	EIS DPV	$1.9 \cdot 10^{-7}$–0.02 $1.5 \cdot 10^{-7}$–0.02	0.08 $3.8 \cdot 10^{-8}$	[22]
SPCE/CNT/AP-NH$_2$/BSA	Covalent by carbodiimide reaction	EDC/NHS (1 h) + Aptamer (12 h) + BSA (1 h)	DPV	0.19–10	0.83	This work

GCE: glassy carbon electrode; BN: boron nitride; CP: capture probe; MCH: 6-mercapto-1-hexanol; CNHs: carbon nanohorns, MOF: Zr-based metal-organic framework, GRN: graphene nanoribbons, cAP-SH: SH-complementary carbendazim aptamer.

3.4. Analysis of CBZ in Tomato

To assess the real-world applicability, the developed aptasensor was used for CBZ detection in tomatoes via a standard addition method. Tomato samples were spiked with 20 μM of CBZ (n = 3), and the concentration detected was 20.93 ± 3.78 μM with RSD of 4.7% and a recovery of 104.7%, demonstrating good precision and accuracy (Table 3).

Table 3. CBZ detection in tomatoes using the proposed aptasensor (n = 3).

Sample	Added (μM)	Found (μM)	RSD (%)	Recovery (%)
Tomato	20.0	20.93 ± 3.78	4.7	104.7

4. Conclusions

In this work, we report for the first time a simple and portable electrochemical aptasensor based on carbon nanotubes for detecting CBZ with LOD values similar to those obtained by HPLC. We developed an electrochemical aptasensor based on carbon nanotubes on a screen-printed carbon electrode (SPCE), where the amino-terminated aptamer was immobilized on the electrode via a carbodiimide reaction. The proposed aptasensor exhibited high selectivity for CBZ compared to interfering agents, good reproducibility (RSD of 2.5%), and a low detection limit (4.35 nM).

The practical application was validated using tomato samples. Therefore, this label-free electrochemical aptasensor offers a simple and reliable method for detecting pesticides in food samples.

Supplementary Materials: The following supporting information can be downloaded at: https://www.mdpi.com/article/10.3390/chemosensors11020117/s1, Figure S1: Bar graph and CVs of electrodes modified with different CNT; Table S1: Data obtained from Figure S1; Figure S2: CVs of electrodes modified with different Nafion concentration; Table S2: data obtained from Figure S2; Table S3: Data obtained for the activation of -COOH by EDC/NHS reaction; Table S4: Data obtained with different concentrations of the aptamer; Table S5: Data obtained with different incubation times of the aptamer; Table S6: Data obtained with different electrodes; Table S7: Data obtained with different binding time of CBZ; Figure S3: Effect of the presence and absence of EDC/NHS in the activation of -COOH.

Author Contributions: Conceptualization, C.J.V. and P.S.-R.; data curation, C.J.V., L.R. and P.S.-R.; formal analysis, C.J.V., L.R. and P.S.-R.; funding acquisition, C.J.V.; investigation, C.J.V. and P.S.-R.; methodology, C.J.V. and P.S.-R.; project administration, C.J.V. and P.S.-R.; resources, C.J.V. and P.S.-R.; supervision, C.J.V. and P.S.-R.; validation, C.J.V., L.R. and P.S.-R.; visualization, C.J.V., L.R. and P.S.-R.; writing—original draft preparation, C.J.V. and P.S.-R.; writing—review and editing, C.J.V. and P.S.-R. All authors have read and agreed to the published version of the manuscript.

Institutional Review Board Statement: Not applicable.

Informed Consent Statement: Not applicable.

Data Availability Statement: The data presented in this study are available in the Supplementary Materials section.

Conflicts of Interest: The authors declare no conflict of interest.

References

1. Cesewski, E.; Johnson, B.N. Electrochemical Biosensors for Pathogen Detection. *Biosens. Bioelectron.* **2020**, *159*, 112214. [CrossRef] [PubMed]
2. Xu, X.; Chen, J.; Li, B.; Tang, L. Carbendazim Residues in Vegetables in China between 2014 and 2016 and a Chronic Carbendazim Exposure Risk Assessment. *Food Control* **2018**, *91*, 20–25. [CrossRef]

3. Liu, J.; Zhang, P.; Zhao, Y.; Zhang, H. Low Dose Carbendazim Disrupts Mouse Spermatogenesis Might Be through Estrogen Receptor Related Histone and DNA Methylation. *Ecotoxicol. Environ. Saf.* **2019**, *176*, 242–249. [CrossRef] [PubMed]
4. Zhou, J.; Xiong, K.; Yang, Y.; Ye, X.; Liu, J.; Li, F. Deleterious Effects of Benomyl and Carbendazim on Human Placental Trophoblast Cells. *Reprod. Toxicol.* **2015**, *51*, 64–71. [CrossRef]
5. Jiang, J.; Wu, S.; Wang, Y.; An, X.; Cai, L.; Zhao, X.; Wu, C. Carbendazim Has the Potential to Induce Oxidative Stress, Apoptosis, Immunotoxicity and Endocrine Disruption during Zebrafish Larvae Development. *Toxicol. Vitr.* **2015**, *29*, 1473–1481. [CrossRef] [PubMed]
6. Zhou, T.; Guo, T.; Wang, Y.; Wang, A.; Zhang, M. Carbendazim: Ecological Risks, Toxicities, Degradation Pathways and Potential Risks to Human Health. *Chemosphere* **2022**, *261*, 137723. [CrossRef] [PubMed]
7. Grujic, S.; Radisic, M.; Vasiljevic, T.; Lausevic, M. Determination of Carbendazim Residues in Fruit Juices by Liquid Chromatography-Tandem Mass Spectrometry. *Food Addit. Contam.* **2005**, *22*, 1132–1137. [CrossRef]
8. Pourreza, N.; Rastegarzadeh, S.; Larki, A. Determination of Fungicide Carbendazim in Water and Soil Samples Using Dispersive Liquid-Liquid Microextraction and Microvolume UV-Vis Spectrophotometry. *Talanta* **2015**, *134*, 24–29. [CrossRef] [PubMed]
9. Ma, C.-H.; Zhang, J.; Hong, Y.-C.; Wang, Y.-R.; Chen, X. Determination of Carbendazim in Tea Using Surface Enhanced Raman Spectroscopy. *Chin. Chem. Lett.* **2015**, *26*, 1455–1459. [CrossRef]
10. Garrido Frenich, A.; Picón Zamora, D.; Martínez Vidal, J.; Martínez Galera, M. Standardization of SPE Signals in Multicomponent Analysis of Three Benzimidazolic Pesticides by Spectrofluorimetry. *Anal. Chim. Acta* **2003**, *477*, 211–222. [CrossRef]
11. Takeda, S.; Fukushi, K.; Chayama, K.; Nakayama, Y.; Tanaka, Y.; Wakida, S. Simultaneous Separation and On-Line Concentration of Amitrole and Benzimidazole Pesticides by Capillary Electrophoresis with a Volatile Migration Buffer Applicable to Mass Spectrometric Detection. *J. Chromatogr. A* **2004**, *1051*, 297–301. [CrossRef]
12. Rezaee, M.; Yamini, Y.; Shariati, S.; Esrafili, A.; Shamsipur, M. Dispersive Liquid–Liquid Microextraction Combined with High-Performance Liquid Chromatography-UV Detection as a Very Simple, Rapid and Sensitive Method for the Determination of Bisphenol A in Water Samples. *J. Chromatogr. A* **2009**, *1216*, 1511–1514. [CrossRef]
13. Gaudin, V. Receptor-Based Electrochemical Biosensors for the Detection of Contaminants in Food Products. In *Electrochemical Biosensors*; Elsevier: Amsterdam, The Netherlands, 2019; pp. 307–365. ISBN 9780128164914.
14. Majdinasab, M.; Mishra, R.K.; Tang, X.; Marty, J.L. Detection of Antibiotics in Food: New Achievements in the Development of Biosensors. *Trends Anal. Chem.* **2020**, *127*, 115883. [CrossRef]
15. Xia, X.; He, Q.; Dong, Y.; Deng, R.; Li, J. Aptamer-Based Homogeneous Analysis for Food Control. *Curr. Anal. Chem.* **2020**, *16*, 4–13. [CrossRef]
16. Oberhaus, F.V.; Frense, D.; Beckmann, D. Immobilization Techniques for Aptamers on Gold Electrodes for the Electrochemical Detection of Proteins: A Review. *Biosensors* **2020**, *10*, 45. [CrossRef] [PubMed]
17. Rapini, R.; Marrazza, G. Electrochemical Aptasensors for Contaminants Detection in Food and Environment: Recent Advances. *Bioelectrochemistry* **2017**, *118*, 47–61. [CrossRef] [PubMed]
18. Li, F.; Yu, Z.; Han, X.; Lai, R.Y. Electrochemical Aptamer-Based Sensors for Food and Water Analysis: A Review. *Anal. Chim. Acta* **2019**, *1051*, 1–23. [CrossRef] [PubMed]
19. Eissa, S.; Zourob, M. Selection and Characterization of DNA Aptamers for Electrochemical Biosensing of Carbendazim. *Anal. Chem.* **2017**, *89*, 3138–3145. [CrossRef]
20. Zhu, C.; Liu, D.; Chen, Z.; Li, L.; You, T. An Ultra-Sensitive Aptasensor Based on Carbon Nanohorns/Gold Nanoparticles Composites for Impedimetric Detection of Carbendazim at Picogram Levels. *J. Colloid Interface Sci.* **2019**, *546*, 92–100. [CrossRef]
21. Wang, R.; Qin, Y.; Liu, X.; Li, Y.; Lin, Z.; Nie, R.; Shi, Y.; Huang, H. Electrochemical Biosensor Based on Well-Dispersed Boron Nitride Colloidal Nanoparticles and DNA Aptamers for Ultrasensitive Detection of Carbendazim. *ACS Omega* **2021**, *6*, 27405–27411. [CrossRef]
22. Khosropour, H.; Maeboonruan, N.; Sriprachuabwong, C.; Tuantranont, A.; Laiwattanapaisal, W. A New Double Signal on Electrochemical Aptasensor Based on Gold Nanoparticles/Graphene Nanoribbons/MOF-808 as Enhancing Nanocomposite for Ultrasensitive and Selective Detection of Carbendazim. *OpenNano* **2022**, *8*. [CrossRef]
23. Cañete-Rosales, P.; Ortega, V.; Álvarez-Lueje, A.; Bollo, S.; González, M.; Ansón, A.; Martínez, M.T. Influence of Size and Oxidative Treatments of Multi-Walled Carbon Nanotubes on Their Electrocatalytic Properties. *Electrochim. Acta* **2012**, *62*, 163–171. [CrossRef]
24. Zhou, J.; Pan, K.; Qu, G.; Ji, W.; Ning, P.; Tang, H. RGO/MWCNTs-COOH 3D Hybrid Network as a High-Performance Electrochemical Sensing Platform of Screen-Printed Carbon Electrodes with an Ultra-Wide Detection Range of Cd(II) and Pb(II). *Chem. Eng. J.* **2022**, *449*, 137853. [CrossRef]
25. Chelly, S.; Chelly, M.; Zribi, R.; Gdoura, R.; Bouaziz-ketata, H.; Neri, G. Electrochemical Detection of Dopamine and Riboflavine on a Screen-Printed Carbon Electrode Modified by AuNPs Derived from Rhanterium Suaveolens Plant Extract. *ACS Omega* **2021**, *6*, 23666–23675. [CrossRef]
26. Tabrizi, M.A.; Acedo, P. Highly Sensitive RNA-Based Electrochemical Aptasensor for the Determination of C-Reactive Protein Using Carbon Nanofiber-Chitosan Modified Screen-Printed Electrode. *Nanomaterials* **2022**, *12*, 415. [CrossRef] [PubMed]
27. Cañete-Rosales, P.; González, M.; Ansón, A.; Martínez, M.T.; Yáñez, C.; Bollo, S. Electrochemical Characterization of Oligonucleotide-Carbon Nanotube Functionalized Using Different Strategies. *Electrochim. Acta* **2014**, *140*, 489–496. [CrossRef]

28. Ruiz-Valdepenas Montiel, V.; Povedano, E.; Vargas, E.; Torrente-Rodríguez, R.M.; Pedrero, M.; Reviejo, A.J.; Campuzano, S.; Pingarrón, J.M. Comparison of Different Strategies for the Development of Highly Sensitive Electrochemical Nucleic Acid Biosensors Using Neither Nanomaterials nor Nucleic Acid Amplification. *ACS Sens.* **2018**, *3*, 211–221. [CrossRef] [PubMed]

29. Serafín, V.; Torrente-Rodríguez, R.M.; González-Cortés, A.; García de Frutos, P.; Sabaté, M.; Campuzano, S.; Yáñez-Sedeño, P.; Pingarrón, J.M. An Electrochemical Immunosensor for Brain Natriuretic Peptide Prepared with Screen-Printed Carbon Electrodes Nanostructured with Gold Nanoparticles Grafted through Aryl Diazonium Salt Chemistry. *Talanta* **2018**, *179*, 131–138. [CrossRef]

30. Lee, J.; Park, I.S.; Kim, H.; Woo, J.S.; Choi, B.S.; Min, D.H. BSA as Additive: A Simple Strategy for Practical Applications of PNA in Bioanalysis. *Biosens. Bioelectron.* **2015**, *69*, 167–173. [CrossRef]

31. Chen, Y.J.; Peng, Y.R.; Lin, H.Y.; Hsueh, T.Y.; Lai, C.S.; Hua, M.Y. Preparation and Characterization of Au/Nipc/Anti-P53/Bsa Electrode for Application as a P53 Antigen Sensor. *Chemosensors* **2021**, *9*, 17. [CrossRef]

32. Farzadfard, A.; Shayeh, J.S.; Habibi-Rezaei, M.; Omidi, M. Modification of Reduced Graphene/Au-Aptamer to Develop an Electrochemical Based Aptasensor for Measurement of Glycated Albumin. *Talanta* **2020**, *211*, 120722. [CrossRef] [PubMed]